Analysis of the incomplete filling of a positive displacement pump due to undissolved gas involving experiments and simulations

Dinghao Pan, Andrea Vacca, and Daniel Gysling

Abstract

The analysis of the incomplete filling behavior of positive displacement machines requires considerations of the undissolved air (i.e. aeration) often associated with uncertainties in the evaluation of the air content within the working fluid and its dependencies with the suction pressure.

This study contributes to this topic by presenting an experimental analysis, as well as modeling considerations, based on an experimental set-up designed by the authors to measure the filling characteristics of an internal gear pump under induced gaseous cavitation. Measurements considered in the study include the pump flow rate vs. shaft speed, as well as the undissolved gas content at the inlet via an innovative solution by CorVera.

Experimental results show that with the same pump inlet pressure, low-speed operations present more tendency for incomplete filling, as compared to higher-speed conditions. This is due to the transient behavior of the air release process in the line connecting the reservoir to the pump, an effect often neglected in similar analyses. This observation is supported by the measured undissolved gas content, which decreases from 7% (at 500 rpm) to 1.5% at 1500 rpm, while the inlet pressure is maintained at 0.3 bar absolute. The measured air release was compared with analytical models, including the equilibrium model and the first-order dynamic model, where a good match was observed between the measurements and the first-order model results produced with an 8 s time constant for fluid with 6 % total air.

The incomplete filling behavior was further examined with a lumped parameter-based simulation model based on the equilibrium fluid model, showing that the total air content at the inlet condition greatly affects the accurate prediction of the pump's incomplete filling. A significant consistency was also found between the measured undissolved air content and the air content values that best predicted the incomplete filling phenomenon.

1 Introduction

Incomplete filling in a positive displacement pump means a situation where the displacement chambers of the pump can no longer be filled with the working fluid in the liquid state. When incomplete filling happens, there are significant volumes of gas in the displacement chambers, which is caused by the working fluid reaching a pressure lower than the saturation pressure (aeration) or, in extreme cases, vapor pressure (vapor cavitation). This phenomenon is associated with volumetric losses (or filling losses), as these gases eventually disappear at the delivery flow. Besides being an energy loss, incomplete filling should also be avoided because it is often associated with detrimental effects such as noise generation or mechanical damages caused by constant bubble collapsing.

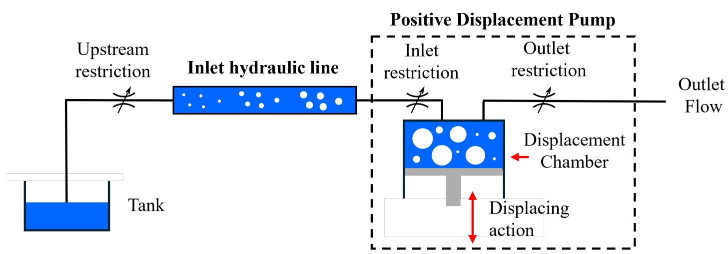

Figure 1: Hydraulic circuit for a positive displacement pump under induced incomplete filling

As Figure 1 illustrates, incomplete filling often occurs under an excessive pressure loss in a) the line connecting the reservoir to the pump inlet (equivalently caused by an upstream flow restriction) or b) between the pump inlet and its displacement chambers (caused both by the pump inlet restriction and the displacement chamber volume expansion related with the displacing action). Therefore, the phenomenon of incomplete filling is related to both the design of the suction circuit and the pump geometry. Certain pump designs are known for having better filling capabilities due to the minimum internal pressure loss while still suffering from incomplete filling under unfavorably high speeds or if an upstream restriction is present. Note that incomplete filling is related to the high operating speeds not only because of a higher pipe loss, but also because of a more rapid volume expansion in the displacement chambers, which gives higher pressure losses in both types a) and b). Additionally, fluid properties, namely the dissolved air content at the reservoir, where saturation conditions can usually be assumed, also heavily affect the incomplete filling behavior due to the effect of aeration. According to Henry-Dalton's law (fraction of air being released is proportional to the absolute liquid pressure if equilibrium), oil that dissolves more air at atmospheric pressure releases more air after the same pressure drop. Incomplete filling may also be caused by entrapped air (pseudo-cavitation), which is not associated with air release but rather with the air leakage into the suction circuit or tank design limitations[1]. Furthermore, an incomplete filling may rise if the reservoir pressure is below the atmosphere. In fact, the incomplete filling issue in aviation lubricating pumps caused by a sub-atmosphere reservoir, known as the "lubrication ceiling", is a crucial consideration in designing aviation pumps[2]. Specifically, this work will neglect pseudo-cavitation phenomena and a sub-atmosphere tank and focus only on incomplete filling caused by the two types of pressure drops a) and b) mentioned above.

Past researchers have studied the pump incomplete filling behavior using experiments and different modeling techniques involving CFD and Lumped Parameter (LP) based models. Both simulation techniques are closely related to an important fluid property parameter known as the "total air". In this paper, "total air" is defined by the volume ratio between the total gas content and the total mixture volume after all dissolved and undissolved gas was separated from the liquid and stored at 1 atmosphere and T_0, which is 0 °C, as Equation (1) states. Note that such a definition is also often considered in engineering modeling utilities, such as Simcenter AMESim[3].

$$x_0 = \frac{V_{gas}(P_{atm}, T_0)}{V_{liq}(P_{atm}, T_0) + V_{gas}(P_{atm}, T_0)} \tag{1}$$

When simulating incomplete fillings, CFD simulations consider the gas presence with two approaches: equilibrium-CFD (where the undissolved gas fraction is determined from the pressure) and dynamic-CFD (which involves additional transport equations for gas or vapor content). Based on equilibrium-CFD, Altare and Rundo [4] showed that, with an unchanged sub-atmospheric pump inlet pressure, higher speeds lead to more severe incomplete filling in a Gerotor. Such speed dependency was also observed in other equilibrium-CFD-based studies, e.g., Hussain et al. for a Gerotor [5], Corvaglia et al. for an external gear pump [6]. Note this speed dependency was reported as negligible by Fresia et al.[7] for an internal gear pump running a high-viscosity fluid. Altare and Rundo noticed a total air setting of 2% in the simulation matched best with closed circuit experiments, indicating that the 7∼11% total air (which is commonly found for open reservoirs[8]) should not be generalized to various circuits. Fresia et al.[7] explained the better matching from the low air content as, before the pump inlet, the pump was only drawing the oil but without separating the air. Furthermore, based on equilibrium-CFD, Boland and Shang [9] studied the incomplete filling scalability, and Rundo et al.[10] investigated the impact of inlet geometries of a vane pump's filling capability under atmosphere inlet pressure. With the dynamic-CFD approach, on the other hand, Buono et al.[11] studied the incomplete filling of a Gerotor, reporting 8% total air simulation matching the measured flow saturation. Similar studies can be found by Stuppioni et al. [12] for a vane pump and by Yin et al. [13] for a piston pump. It should be pointed out that popular dynamic-CFD models, such as the 'full cavitation model' introduced by Singhal et al.[14], often require empirical time constants to describe the speed of phase change processes, including vaporization/condensation and aeration/dissolution. Early experiments from Schweitzer and Szebehely[8] reported $\mathcal{O}(10^1)$ second half release time for dissolved air in hydraulic oils. Measurements from Kowalski et al.[15] showed that air release is much slower than vaporization if water is below vaporization pressure, and Yang et al. [16] reported that dissolution is further slower than the air release for the same pressure differential. Notable simulation-based work from Stuppioni et al.[17, 12] investigated how the outlet flow and pressure ripple of a pump with atmospheric inlet pressure could change under different time constant settings in the dynamic-CFD framework, reporting air release time $\mathcal{O}(10^{-2})$ and dissolution time $\mathcal{O}(10^0)$ matched best with measurements, and concluding these time constants as critical for describing the gas dynamics in the simulations. More details on different dynamic-CFD models can be found in the review paper from Orlandi et al.[18].

In studies that investigated the incomplete filling behavior with the LP simulation approach, there is also the static cavitation model (where the fractions of vapor and released gas are pressure-dependent) and the dynamic cavitation approach (where the vapor and released gas fraction are solved from the rate equations). Casoli et al. [19] formulated a static model to consider the fluid property change under sub-atmosphere conditions and noticed both a higher total air content and a higher saturation pressure emphasized the incomplete filling prediction. Vacca et al.[20] used a similar implementation to study the incomplete filling behavior of an axial piston pump, discussing the necessity of tuning the model parameters to achieve a higher fidelity compared to experiments. Also based on a static model, Pleskun et al.[21] reproduced the incomplete filling behavior for a screw pump. On the other hand, dynamic cavitation models have recently been explored for LP simulations, as can be found in the work from Zhou et al.[22], Shah et al.[23], and Mistry and Vacca[24], involving similar time constants discussed for dynamic-CFD as well. The work from Rundo et al. [25] detailed these time constants based on pump flow and pressure ripples and suggested release time $\mathcal{O}(10^{-3})$ and dissolution time $\mathcal{O}(10^1)$ for pumps with atmospheric inlet pressure. However, relevant studies on the incomplete filling behavior have not yet been presented from LP simulations based on dynamic cavitation considerations.

Previous studies on pump incomplete filling often focused on the pump side and didn't quantify the impact of the two types of pressure drops illustrated in Figure 1. Additionally, although past incomplete filling simulations have widely investigated the fluid settings such as total air and their effects on prediction accuracy, whether the best-matching fluid parameters (total air) can be justified with the design of the circuit has not been understood.

To investigate the incomplete filling behavior of a positive displacement pump, a test rig was set up in the authors' research lab to consider the two stages of pressure drops illustrated in Figure 1. Different operating speeds were measured, including the measurement of the delivery flow, the pressure at the pump inlet, and the gas void fraction (GVF) in the hydraulic line before the pump inlet. The amount of gas content measured at the pump inlet was compared to the prediction from a first-order air release model. Furthermore, static cavitation-based simulations that utilize different total air settings were used to investigate the pump's incomplete filling behavior. The influence of total air setting will be discussed and compared with the total air which can be deduced from the gas content measurements. The comparison, as will be shown later, underscores the importance of both the inlet pressure and the total air in achieving good accuracy in predicting the incomplete filling phenomenon.

2 Experimental study on incomplete filling

2.1 Experimental set up

The setup for measuring the incomplete filling behavior for a reference 8 cc/rev internal gear pump [26] is illustrated in Figure 2. **Valve 1** regulates the pump inlet pressure, and **valve 2** is set to fully open to minimize the pressure load on the pump outlet. Such arrangements minimize the effect of pump internal viscous leakage when quantifying the incomplete filling. The test setup also includes an air valve, which was constantly closed during the test. Such a valve allows tests with entrained air, which will be the subject of future work. Pressure sensors $\boldsymbol{P}_1$ and $\boldsymbol{P}_2$ measure the pressure change along the hydraulic lines (**HL1** and **HL2**). More details regarding the components used in the measurements are given in Table 1.

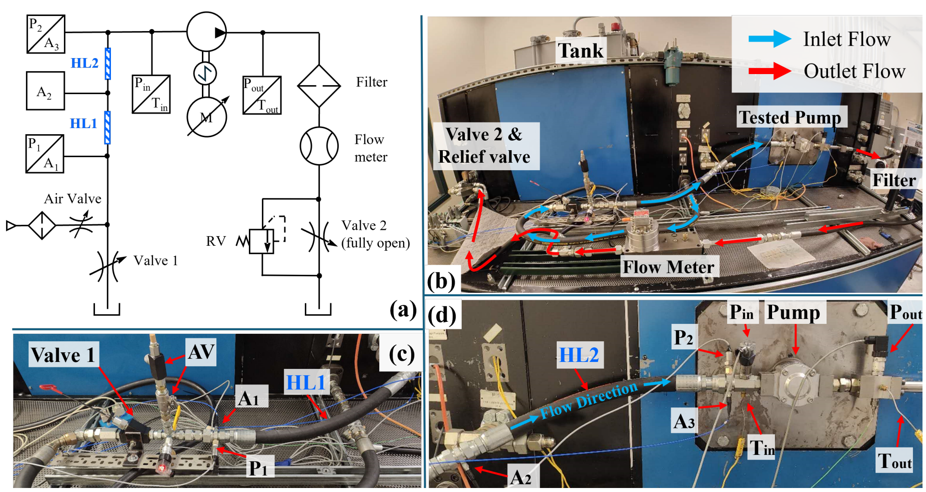

Figure 2: Test circuit to measure the incomplete filling behavior
(a: hydraulic circuit; b: overlook of the entire setup; c: inlet region; d: tested pump)

Components	Parts used	Accuracy
Pump	Eckerle EIPS2-008	N/A
Valve 1	Sun Hydraulics NFDD-KGN	N/A
Flow meter	VSEflow VS 2EPO 12V	0.3% measured value
P_{in}	WIKA S-20-1.6	0.003 bar
P_{out}	HAD 4745-B-006-00	0.25% measured value
A_1,A_2,A_3	PCB 102A44	0.07 bar
P_1,P_2	Keller America absolute type	0.25% measured value
HL1,HL2	DIN EN 856, inner diameter 1 inch, pipe length 2 feet	
Tank	Contains $\sim$ 290 liter hydraulic fluid	

Table 1: Component used in the test circuit

Notably, this work utilizes a non-intrusive, in-line, real-time, SONAR-based measurement system to quantify the gas void fraction (GVF) in the fluid entering the pump inlet. Based on beam-forming principles, the measurement system calculates the fluid's speed of sound utilizing the output of three acoustic pressure sensors ($\boldsymbol{A}_1$, $\boldsymbol{A}_2$, $\boldsymbol{A}_3$). The measured sound speed is then interpreted in terms of the gas void fraction utilizing Wood's equation[27]. For clarity, the GVF measured here is defined as the ratio of the gas volume to the total fluid volume. Note that this differs from the volumetric ratio between the gaseous and mixture flow rates. However, for homogeneous conditions where the velocity of the gas phase approaches that of the liquid phase (generally true for low GVF scenarios), the two definitions become equivalent. More details on the measurement approach can be found in Gysling[28].

2.2 Operating conditions

ISO-VG 46 hydraulic oil was used during the test, and measurements were taken at 23 °C inlet and outlet temperature. Four operating speeds (500, 1000, 1500, 2000 rpm) were tested with different pump inlet pressures (measured by $\boldsymbol{P}_{in}$), which were regulated by **valve 1**. During the test, a loud hissing noise was heard when the pump inlet pressure fell below $\sim$ 0.2 bar absolute, with spatial location near the outlet port on the pump body. Such pressure limit appeared to be lower for the low-speed conditions: for 500 rpm such limit was $\sim$ 0.18 bar absolute, whereas for 2000 rpm the limit was $\sim$ 0.3 bar absolute. The noise was believed to be related to the fierce vapor bubble collapsing process on the pump outlet side. All measurements discussed in this work are above this low pressure limit, to avoid extended pump operation in the possible damaging conditions.

The increase of the pump outlet pressure with the operating speed shown in Figure 3 is caused by the pressure loss characteristics of the outlet circuit. According to the pump specs [26], at 1500 rpm there is a decrease of volumetric efficiency of 0.2% every 8 bar of outlet pressure increase. This justifies that the effect of the measured increase of outlet pressure on the measured volumetric

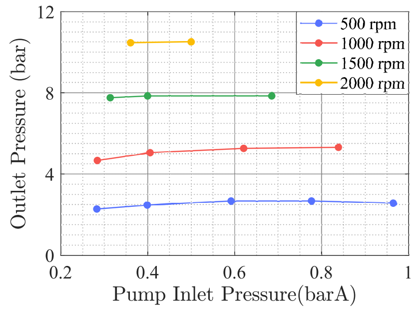

Figure 3: Pump outlet pressure

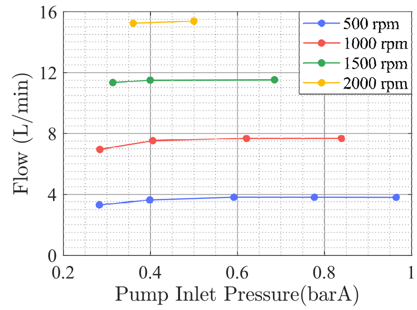

Figure 4: Pump Outlet flow

efficiency is minor, and major volumetric efficiency loss in the measurements should be associated with the incomplete filling phenomenon.

2.3 Incomplete filling flow measurement

As plotted in Figure 4, for constant operating speed, the measured pump outlet flow decreases with a lower pump inlet pressure. Significant flow rate drops happen at pressure values close to the limiting pressure ranges. The impaired outlet flow represents the incidence of incomplete filling inside the pump, which can be seen more clearly from the volumetric efficiency evaluated in Figure 5.

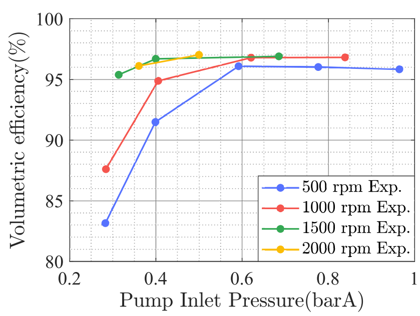

Figure 5: Volumetric efficiency

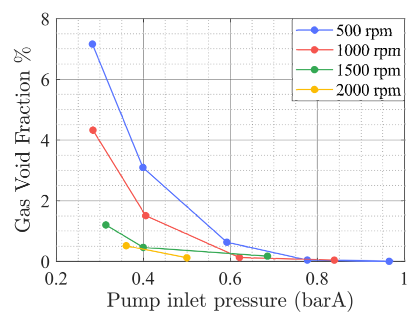

Figure 6: Measured GVF

Figure 5 shows an interesting trend where, as the speed increases from 500 to 2000 rpm, the incomplete filling becomes less obvious for the same inlet pressure. This trend appears to be in contrast with the common belief that higher speeds promote incomplete filling, as reported in several sources [1, 29] and recent works by Rundo[4] and Corvaglia et al.[6]. However, this paper will show how this trend does not contradict, but rather complement, the common understanding of incomplete filling. As mentioned in the first section, incomplete filling is caused by the behaviors of both the inlet circuit and the pump design. In this test, the effect of the inlet circuit prevails, generating such a trend.

2.4 Gas content measurement

The Gas Void Fraction(GVF) measured with the CorVera system is plotted in Figure 6. Note the raw GVF was calculated by the measurement system around every 2 seconds, which involves instantaneous oscillations of absolute standard deviation $\sim$ 0.25%. The data reported in Figure 6 averaged a 2-minute period after the on-screen measurement stabilized (which takes about 1 minute). It should be carefully noted that the measured GVFs represent the volume of air at sub-atmospheric pressures, not the atmosphere pressure. Also note that the measured GVF can be considered as an averaged measurement at the middle position between hydraulic lines **HL1** and **HL2**, and the gaseous volume entering the pump inlet should be higher than the measured GVF, as the air release process develops along the length of the hydraulic lines.

The figure shows that as the operating speed increases, the gas volume in the inlet hydraulic lines becomes significantly lower. This trend can be explained as follows: for low speeds, due to the lower mean velocity, the fluid takes a longer time to pass the inlet hydraulic line (see Figure 1), and more air is therefore released into the fluid.

The GVFs for 1500 and 2000 rpm shown in Figure 6 give a clear clue about the low amount of released air at the pump inlet, which supports the assumption raised by Fresia et al.[7] that under higher flowrates very least air bubbles are released into the fluid before the pump inlet. This assumption well explains why equilibrium-CFD requires a lower total air setting to reproduce the incomplete filling. Particularly, for 500 rpm operating speed, it takes $\sim$ 10 seconds for the fluid to pass the total two hydraulic lines, whereas, for 2000 rpm, the travel time becomes $\sim$ 2.4 seconds. Such difference in the travel time indicates that the time scale of the air release process is on the order of magnitude of seconds, which is consistent with the value found in the measurements by Schweitzer and Szebehely[8]. Note Rundo et al.[25] and Stuppioni et al.[12] reported very fast air release constants ($10^{-2} \sim 10^{-3}$) that predicted experiment-matching pump outlet pressure ripples; however, we believe the time constants discussed in their work are more related to the fluid-dynamic process inside the pump domain (their work investigated pump with atmospheric inlet pressure), and the process of air release in the circuit upstream the pump inlet should involve a different time constant that is slower, because of less volume expansion or boundary perturbation in the region.

3 Analytical models of air release

3.1 Equilibrium fluid model

The air release measured can be compared with the results from an equilibrium fluid model, which states whenever a pressure change happens to the fluid, the air release and the volume change of the mixture are achieved instantly so that the fluid is always in the equilibrium state. Studies such as [10] and [19] have reported that the fluid equilibrium model when properly tuned, can give a good prediction for the incomplete filling behavior in positive displacement machines. According to the equilibrium fluid model, the volume of the air undissolved from the fluid (under the equilibrium state) $V_{g,undis,eq}$ can be determined according to Henry's law, as equation (2) gives. $P_{vap,H}$ is the high vaporization pressure [19]. P_{sat} is the saturation pressure above which all air is dissolved. Note equation (2) applies when the fluid pressure is between $P_{vap,H}$ and P_{sat} and if the fluid pressure is beyond the range, all or none air is released.

$$\frac{V_{g,undis,eq}(P_{sat},T_0)}{x_0/(1-x_0)\cdot V_{liq}} = \frac{P_{sat}-P}{P_{sat}-P_{vap,H}} \tag{2}$$

The volume of the undissolved air evaluated in Equation (2) must be evaluated at the reference state (P_{sat}, T_0), as Henry's law quantifies about the amount of substance rather than the volume. The gas volume expansion caused by pressure decrease can be evaluated with equation (3) for a given polynomial coefficient κ, which is taken as 1.3 in this work. Note the temperature of the left-hand side fluid in equation (3) can be solved from κ based on the ideal gas law and is fundamentally different from the liquid temperature.

$$V_{g,undis,eq}(P) = \left(\frac{P_{sat}}{P}\right)^{1/\kappa} V_{g,undis,eq}(P_{sat},T_0) \tag{3}$$

3.2 Dynamic air release model

The equilibrium fluid model assumes the air release process to happen instantly, whereas in reality, such equilibrium takes time to achieve. In fact, the air release process in hydraulic oils has been reported to have a proportional relationship with the extent of phase imbalance [8]. Based on this idea, a first-order model is often used to study the transient air release in fluid, of which the applications can be found in Simerics MP+[12], ANSYS CFX [16], and AMESim[3, 25].

The key idea of the first-order air release model can be expressed in the Lagrangian form for a moving fluid element with a specific mass δM (no mass transfer between surrounding fluid elements), as equation (4) gives. In the equation, $V_{g,undis}(t;P)$ is the volume of the gas released into the fluid element after time t (at $t = 0$ no air is released) under pressure P. $V_{g,undis,eq}(P)$ is the equilibrium volume solved from equation (3). Equation (4) can also be alternatively expressed with mass terms; however, since the thermodynamic conditions are unified, the two ways of expression are equivalent. From equation (4), the volume of released air can be solved, as equation (5) gives, based on which the instantaneous void fraction f_{void} can be thus calculated by equation (6).

$$\left.\frac{dV_{g,undis}(t;P)}{dt}\right|_{\delta M} = \frac{V_{g,undis,eq}(P) - V_{g,undis}(t)}{\tau} \tag{4}$$

$$V_{g,undis}(t;P) = (1 - e^{(-t/\tau)}) \cdot V_{g,undis,eq}(P) \tag{5}$$

$$f_{void}(t;P) = \frac{V_{g,undis}(t;P)}{V_{g,undis}(t;P) + V_{liq}(P)} \tag{6}$$

Using a time constant $\tau = 8$ second, the transient gas void fractions were solved for a fluid with 6% total air (x_0) at different sub-atmospheric pressures, and results are plotted in Figure 7. Evident trends from the figure are: more air is released with time progressing; for a specific pressure, the rate of air release slows down with time; and the lower the pressure, the more air is released after the same amount of time. It should also be mentioned that if the pressure change caused by the air release is neglected, the air release process in the fluid that travels along the hydraulic lines can be predicted with constant-pressure curves given in Figure 7. Indeed, the inlet pressure change along the pipe was found to be low, as Figure 8 shows.

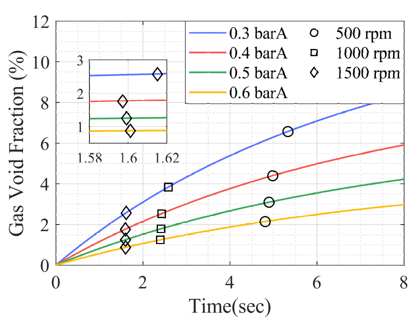

Figure 7: Void fraction predicted with 1^{st} order air release ($x_0 = 6\%, \tau$=8s)

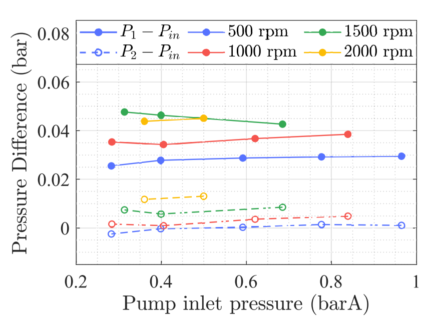

Figure 8: Measured inlet line pressure change ($\boldsymbol{P}_1$: pipe enter, $\boldsymbol{P}_2$: pipe end)

Apparently, the choice of τ affects the calculation in Equation (6): higher τ slower the air release, and it was noticed that a $\tau = 8$ provides the best consistency with experiments. Specifically, the markers in Figure 7 highlight the predicted gas void fractions at the middle length of the hydraulic line (middle between **HL1** and **HL2**). The predicted GVF values are found to be consistent with the measured GVFs shown in Figure 6. Certain errors in the low GVF region can be explained by the first order being less accurate when the GVF is low, as a smaller bubble size hinders the air release process.

It is worth mentioning that computing the fluid travel time for the markers in Figure 7 involved two counter-acting considerations. On one hand, there is the compressibility-accelerate effect: air release along the pipe causes density to decrease, and to fulfill mass conservation, the flow is accelerated. The flow travel distance L after time t can be determined based on the void fraction history in the fluid element, as equation (7) gives by assuming the fluid starts from a location where no air is released. $\bar{u}_0$ is the mean flow velocity calculated based on the measured flow rate. This mean velocity is considered to happen at the starting location of the hydraulic pipe, assuming the density variation at the position to be negligible due to a minimal air release.

$$L(t) = \int_0^t \frac{\bar{u}_0}{1 - f_{void}(t)} dt \tag{7}$$

On the other hand, the incomplete-filling-decelerate effect also affects the evaluation of the travel time, where since a lower inlet pressure promotes incomplete filling, the mean velocity $\bar{u}_0$ which is calculated from the measured flow rate drops, thus giving a longer time for the fluid to reach the same distance. It was observed that such the incomplete-filling-decelerate effect wins over the compressibility-accelerate effect for 500 and 1000 rpm, explaining why for these speeds, the travel time for the fluid to reach the middle of the hydraulic lines becomes longer when the pump inlet pressure decreases. For 1500 rpm, on the other hand, Figure 7 shows that as the pressure decreases, the travel time first decreases and then increases. Such behavior is caused by a weaker incomplete-filling-decelerate effect under 1500 rpm, which loses its dominance to the compressibility-accelerate effect in higher pressure ranges.

4 Equilibrium-fluid-based pump simulation

4.1 Simulation setup and settings

The reference pump tested is a crescent-type internal gear pump with involute-type gear profiles. To study the pump incomplete filling behavior, isothermal lumped parameter-based pump simulations based on the circuit shown in Figure 9 were performed, considering the fluid with the equilibrium fluid model. In the simulation, the outlet pressure uses the measured values. The simulation model is a simplified version of a more complex model from the authors' previous work[30]. Particularly, the model used here neglects the viscous leakage in the fluid films and across gear tips, since the outlet pressure was low. Radial micro-motion on the gear set was considered, as it affects the gear center distance and, hence, the effective displacement. The micro-motions of the two gears are solved based on the Ocvirk solution[31], considering both hydrostatic and contact loadings on the gear set[30]. More details on the coupled pump simulation model can be found in the authors' previous works[32, 30].

The pump was simulated up to 6 shaft revolutions, and the outlet flow rate averaged from the last 3 gear teeth period was considered to study the incomplete filling behavior. With such a time window, all performed simulations reported an absolute residue of less than 0.02 % in the volumetric efficiency. More details on the simulation settings can be found in table 2.

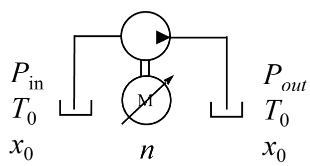

Figure 9: Simulated circuit

Sim. setting	**Value**
Fluid	ISO-VG46
$P_{vap,H}$	0.22 barA
P_{sat}	1 atm
T_0	23 $°C$

Table 2: Simulation settings

4.2 Effect of total air in predicting incomplete filling

The pump volumetric efficiencies predicted by the simulation model considering different total air settings are compared with the measurements in Figure 10 for the four measured operating speeds.

Figure 10 shows a significant trend: for low speed (500 rpm) and low inlet pressure (0.3, 0.4 bar absolute), a higher total air gives a more accurate prediction in the impaired volumetric efficiency. When the inlet pressure is not very low (> 0.6 bar absolute), low total air simulation gives better predictions. The trend also appears for 1000 rpm as the figure shows, whereas for higher speeds 1500 rpm and 2000 rpm, this trend was not observed. Instead, for the high speeds, simulation with very low total air appeared to match best with the measured volumetric efficiencies.

The underlying physics in different total air settings can be understood as follows. Due to the equilibrium fluid assumption, when the fluid pressure is below saturation, more air is released into a fluid if the fluid is defined with a higher total air. The higher amount of undissolved air leads to a lower bulk modulus of the fluid mixture, hence giving more density drops when the volume expansion happens inside the pump inlet and consequently a lower volumetric efficiency. On the other hand, the fact that such a trend is not evident for high speeds (1500, 2000 rpm) is that not much air was released for the speeds, which can be confirmed with the measurements in Figure 6.

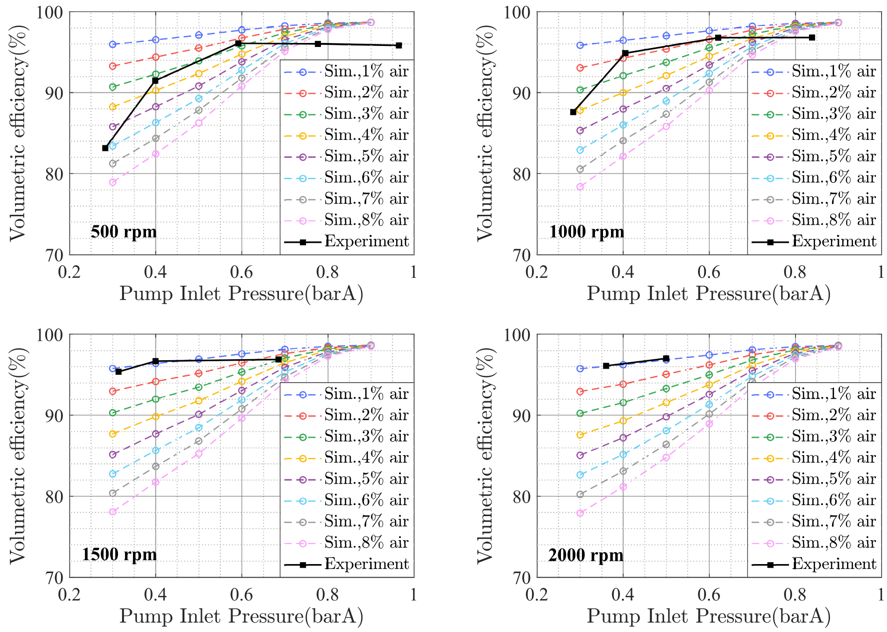

Figure 10: Measured pump volumetric efficiency compared with simulation results predicted based on fluids with different total air values

4.3 Speed dependency at higher speeds

As mentioned in section 2.3, Rundo et al.[10] and Corvaglia et al.[6] once noticed that for the same sub-atmosphere inlet pressure, the higher the operating speed, the more severe the incomplete filling becomes. Actually, such speed dependency can be reproduced from the simulation model used in this paper as well, as Figure 11 shows: for a certain total air, the pump volumetric efficiency drops with a higher speed, indicating a more severe incomplete filling. This speed dependency observed by earlier researchers can be explained as follows. As the flow rate becomes substantially high, the time for air release to happen becomes trivial such that only a very tiny amount of air can be released into the fluid before the pump inlet. Because the volume expansion process in the displacement chamber happens much faster ($\mathcal{O}(10^{-3}) \sim \mathcal{O}(10^{-2})s$) than the air release process ($\mathcal{O}(10^{1})$ s), the fluid that enters the pump, which is off-equilibrium (concerning the air release process), will not change its off-equilibrium status during the volume expansion stage. Such behavior gives a good rationale for considering the off-equilibrium fluid at the pump inlet as an "equivalent fluid" with less total air in the state of air-release equilibrium. In this way, for high-speed operations, the "equivalent fluids" that enter the pump inlet can be considered as not changing between different operating speeds, as they all equivalently contain a very small amount of total air. In this situation, therefore, the primary cause of the incomplete filling becomes the pressure drop inside the gear displacement chambers, which is related to the volume expansion. Since a higher speed raises the expansion rate, a higher pressure drop can be expected in the displacement chambers and hence increases the volumetric loss for a higher operation speed.

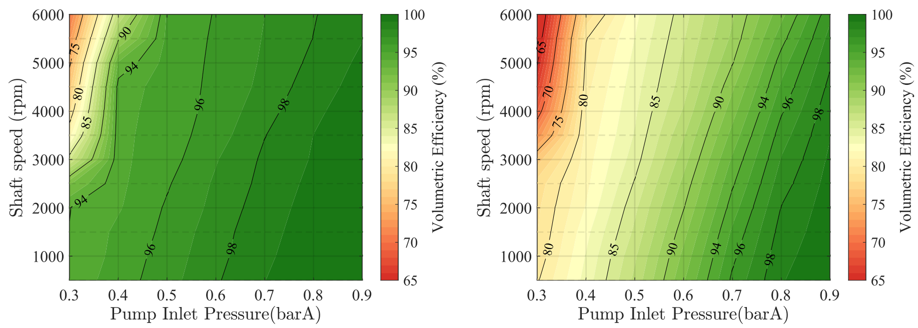

Figure 11: Simulated volumetric efficiency of a wider speed range (left: with 2% total air, right: with 8% total air)

The reason why such speed dependency seems to be reversed for lower speeds (see discussion in section 2.3) is as follows. A lower speed operation gives the fluid more time to release air; hence, the "equivalent fluid" that enters the pump inlet at low speeds has a significantly higher amount of total air when compared to the "equivalent fluid" at high speeds. This means that for a specific inlet pressure where incomplete filling happens, the pump volumetric efficiency should first increase and then decrease. Take 0.3 bar absolute pump inlet pressure shown in figure 11 as an example, when the speed increases from 500 rpm to 2000 rpm, the volumetric efficiency of a pump that is under incomplete filling condition should be first referred to a volumetric efficiency map predicted with a higher total air (e.g., 8 % in the right figure, where a low volumetric efficiency would be found) and then a map with a lower total air (e.g., 2% in the left figure, which gives a higher volumetric efficiency compared to the 8% map for the same speed). In the low-speed domain, the difference in the amount of air that is released into the upstream fluid is the main driving force in determining the incomplete filling, because the fluid compressibility upstream the pump inlet significantly varies in this speed domain. As the operating speed increases from 2000 rpm to higher, the map from where an accurate volumetric efficiency can be found gradually converges towards a map predicted with a trivial amount of total air (e.g., 2 % in the left figure), so that a higher speed gives a lower volumetric efficiency, due to a higher pump internal pressure drop becoming the dominant force in defining the incomplete filling phenomenon.

4.4 Air content comparison with measurement

The fluid at the pump inlet may carry a higher volume of released air than the measured value, which is a type of averaged GVF over the complete hydraulic lines. The increase in the GVF between the measured value and the value that should be expected at the pump inlet can be described with a factor. At first thought this factor should be slightly lower than 2 due to the non-linearity shown in Figure 7, but on the other hand, the non-linearity of the speed of sound (based on which the GVF is measured) with the gas presence involves an opposite effect which raises the factor. A more rigorous discussion on this factor is beyond the scope of this work. In this work, we assume the factor to be 2 for convenience.

In this way, the total air in the “equivalent fluid” at the pump inlet can be evaluated by back calculating x_0 from (3) and (2) where twice the measured GVF is used as the starting $V_{g,undis,eq}(P)$ value. Meanwhile, the equilibrium-state gas void fraction predicted from the equilibrium fluid model is given in Figure 12 so that the back-calculation can be conveniently achieved by looking up from the figure.

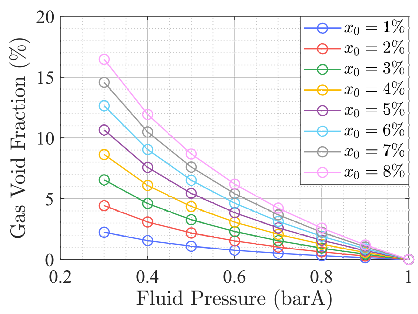

Figure 12: Equilibrium-state gas void fraction in sub-atmospheric fluids with different total airs

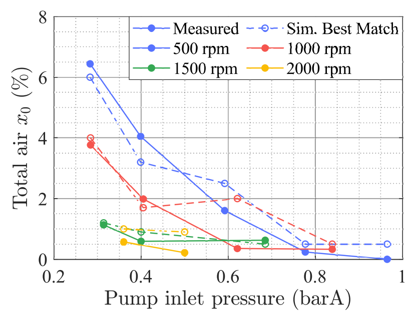

Figure 13: “Measured equivalent” versus “simulation proposed” total air

The total air in the “equivalent fluid” calculated from the measured GVF results is plotted in 13, labeled as “measured equivalent” total airs. Also plotted in Figure 13 are the “simulation proposed” total airs: the total air that gives the best volumetric efficiency predictions from the simulation which can be inferred from Figure 5. To account for possible inaccuracy in volumetric efficiency evaluations under higher inlet pressure conditions ($\geq$ 0.6 bar absolute), the “simulation proposed” total air is picked as 0.5 % in the higher pressure range. The comparison in Figure 13 gives a significant consistency between the “measured equivalent” and “simulation proposed” total air. Such consistency once again supports the validity of the gas void fraction measurements and also supports the earlier assumption stating that off-equilibrium fluid entering the pump inlet can be equivalently viewed as a fluid with a lower total air under the equilibrium state.

Another important consideration can be made from Figure 13: the total air setting in pump incomplete filling simulations is an important and uncertain parameter that should be carefully considered based on the inlet circuit design. For higher flowrates or shorter inlet lines where less air release is expected, a lower total air might be accurate; however, when the air release upstream the pump is not negligible, the total air setting greatly affects the accuracy in predicting the incomplete filling behavior. Notably, our work not only identified the importance of the total air parameter but also for the first time measured its physical value in incomplete filling studies. This breakthrough suggests a promising direction for conditioning the inlet settings in future studies on positive displacement pumps, whether in simulation or tests.

5 Conclusion

This paper presented a study on the incomplete filling phenomenon of a positive displacement pump.

The study first experimentally investigated the reference pump incomplete filling under different inlet pressure and speed conditions. The measurements were achieved via a novel test rig setup in the authors' research lab, where two stages of pressure drops, including an upstream orifice and the pump internal inlet pressure drop, were simultaneously investigated. The measurement setup highlights an in-line gas void fraction measurement, the first time for an incomplete filling study to measure the fluid property that enters the pump inlet.

Measurements showed clear signs of incomplete filling when the pump inlet was subject to sub-atmosphere pressures. The measurements unveils the two factors that influence the incomplete filling characteristics of a pump:

(1) In the low speed operating domain, the amount of air released into the fluid upstream the pump inlet is the main driving force in determining the incomplete filling, as the fluid compressibility significantly varies in this speed domain. Since a lower speed gives more time for the air to release into the fluid before the pump inlet, a lower speed leads to a more severe incomplete filling.

(2) In the high speed operating domain, the pump inlet fluid contains a very small amount of undissolved air, so that the fluid compressibility becomes less important. Instead, the higher volume expansion rate inside the pump displacement chambers leads to a higher pressure drop in the displacement chambers, which predominantly defines a more severe incomplete filling situation.

This study also utilized simulations to study the incomplete filling behavior, involving a transient first order air release model to investigate the air release process in the pipe and an equilibrium-fluid-based LP pump simulation model to investigate the pump's volumetric performance under incomplete filling.

The first order air release model with 6% total air and 8 second air release time constant showed a good accordance with the measured gas void fraction, supporting the validity of both the model and the gas void fraction measurements in studying the air release process in hydraulic lines.

Results from the equilibrium-fluid-based LP pump simulation showed that the total air setting greatly affects the prediction of the pump incomplete filling. Specifically, for low speed low inlet pressure conditions, simulation with higher total air gives more accurate volumetric efficiency predictions. The "equivalent" total air at the pump inlet, derived from the gas void measurement, was found to match well the total air settings that give the most accurate incomplete filling predictions. This finding confirms the importance of the total air, and also validates a crucial assumption that a fluid that has not reached air-release equilibrium at the pump inlet can be equivalently considered as a different fluid with less total air in the state equilibrium, and they can give the same effective prediction for the incomplete filling phenomenon. Notably, this work not only identified the importance of the "equivalent" total air concept but also measured it for the first time in incomplete filling studies. This breakthrough suggests a promising direction for conditioning the inlet settings in future studies on positive displacement pumps, whether in simulation or tests.

Acknowledgement

The authors would like to thank Prithvi Chandiramani, Seshan Suresh, and David Johnson for the inspiring discussions and valuable technical advice.

References

[1] Andrea Vacca and Germano Franzoni. *Hydraulic fluid power: fundamentals, applications, and circuit design*. John Wiley & Sons, 2021. ISBN: 978-1-119-56910-7.

[2] P. H. Schweitzer. "Effect of Aeration on Gear-Pump Delivery and Lubrication Ceiling". In: *Transactions of the American Society of Mechanical Engineers* (1945). DOI: 10.1115/1.4018189.

[3] Siemens PLM Software Inc. *Simcenter Amesim™ software User's guides: AHYD Advanced Fluid Properties Technical bulletin no. 117*. 2021.

[4] Giorgio Altare and Massimo Rundo. "Computational Fluid Dynamics Analysis of Gerotor Lubricating Pumps at High-Speed: Geometric Features Influencing the Filling Capability". In: *Journal of Fluids Engineering* (2016). DOI: 10.1115/1.4033675.

[5] Tarique Hussain et al. "A Simulation Study of Lubricating Oil Pump for an Aero Engine". In: *Journal of Mechanical Engineering (JMechE)* (2021). DOI: 10.24191/jmeche.v18i3.15417.

[6] Alessandro Corvaglia et al. "Simulation and Experimental Activity for the Evaluation of the Filling Capability in External Gear Pumps". In: *Fluids* (2023). DOI: 10.3390/fluids8090251.

[7] Paola Fresia et al. "CFD Modelling of an Internal Gear Pump for High Viscosity Fluids". In: *International Design Engineering Technical Conferences and Computers and Information in Engineering Conference*. 2023. DOI: 10.1115/DETC2023-111589.

[8] P. H. Schweitzer and V. G. Szebehely. "Gas evolution in liquids and cavitation". In: *Journal of Applied Physics* (1950). DOI: 10.1063/1.1699579.

[9] Hannah Boland and Lizhi Shang. "An Analysis of Cavitation Phenomena Scalability in Axial Piston Machine". In: *ASME/BATH 2023 Symposium on Fluid Power and Motion Control*. 2023. DOI: 10.1115/FPMC2023-113585.

[10] Massimo Rundo, Giorgio Altare, and Paolo Casoli. "Simulation of the filling capability in vane pumps". In: *Energies* (2019). DOI: 10.3390/en12020283.

[11] Dario Buono et al. "Modelling Approach on a Gerotor Pump Working in Cavitation Conditions". In: *Energy Procedia* (2016). DOI: 10.1016/j.egypro.2016.11.089.

[12] Umberto Stuppioni et al. "Computational Fluid Dynamics Modeling of Gaseous Cavitation in Lubricating Vane Pumps: On Metering Grooves for Pressure Ripple Optimization". In: *Journal of Fluids Engineering* (2022). DOI: 10.1115/1.4056416.

[13] Fang-long Yin et al. "Numerical and experimental study of cavitation performance in sea water hydraulic axial piston pump". In: *Proceedings of the Institution of Mechanical Engineers, Part I: Journal of Systems and Control Engineering* (2016). DOI: 10.1177/0959651816651547.

[14] A.K. Singhal et al. "Mathematical Basis and Validation of the Full Cavitation Model". In: *Journal of Fluids Engineering* (2002). DOI: 10.1115/1.1486223.

[15] Karoline Kowalski et al. "Experimental Study on Cavitation-Induced Air Release in Orifice Flows". In: *Journal of Fluids Engineering* (2018). DOI: 10.1115/1.4038730. URL: https://doi.org/10.1115/1.4038730.

[16] HQ Yang, AK Singhal, and M Megahed. "The full cavitation model". In: *Lecture seires - Von Karman Institute for fluid dynamics* 4 (2005). purchased on 2020 Sept. from VKI store, p. 10.

[17] Umberto Stuppioni et al. "Computational Fluid Dynamics Modeling of Gaseous Cavitation in Lubricating Vane Pumps: An Approach Based on Dimensional Analysis". In: *Journal of Fluids Engineering* (2020). DOI: 10.1115/1.4046480.

[18] Francesco Orlandi, Luca Montorsi, and Massimo Milani. "Cavitation analysis through CFD in industrial pumps: A review". In: *International Journal of Thermofluids* (2023). DOI: 10.1016/j.ijft.2023.100506.

[19] Paolo Casoli et al. "Modelling of fluid properties in hydraulic positive displacement machines". In: *Simulation Modelling Practice and Theory* (2006). DOI: 10.1016/j.simpat.2006.09.006.

[20] Richard Klop Andrea Vacca and Monika Ivantysynova. "A Numerical Approach for the Evaluation of the Effects of Air Release and Vapour Cavitation on Effective Flow Rate of Axial Piston Machines". In: *International Journal of Fluid Power* (2010). DOI: 10.1080/14399776.2010.10780996.

[21] H Pleskun, A Syring, and A Brümmer. "Transient chamber filling in rotary positive displacement vacuum pumps". In: *IOP Conference Series: Materials Science and Engineering* (2022). DOI: 10.1088/1757-899X/1267/1/012016.

[22] Junjie Zhou, Andrea Vacca, and Bernhard Manhartsgruber. "A Novel Approach for the Prediction of Dynamic Features of Air Release and Absorption in Hydraulic Oils". In: *Journal of Fluids Engineering* (2013). DOI: 10.1115/1.4024864.

[23] Yash Girish Shah, Andrea Vacca, and Sadegh Dabiri. "Air Release and Cavitation Modeling with a Lumped Parameter Approach Based on the Rayleigh–Plesset Equation: The Case of an External Gear Pump". In: *Energies* (2018). DOI: 10.3390/en11123472.

[24] Zubin Mistry and Andrea Vacca. "Cavitation Modeling Using Lumped Parameter Approach Accounting for Bubble Dynamics and Mass Transport Through the Bubble Interface". In: *Journal of Fluids Engineering* (2023). DOI: 10.1115/1.4062135.

[25] Massimo Rundo, Raffaele Squarcini, and Francesca Furno. "Modelling of a Variable Displacement Lubricating Pump with Air Dissolution Dynamics". In: *Source: SAE International Journal of Engines* (2018). DOI: 10.4271/03-11-02-0008.

[26] Eckerle Technologies GmbH. *EIPS segment pump - industrial design*. 2023. URL: https://eckerle.com/en/products/eips2-008ra04-1x-s111-eips-segment-pump-industrial-design.

[27] Albert Beaumont Wood and RB Lindsay. *A textbook of sound*. 1956.

[28] Daniel L. Gysling. "Accurate mass flow and density of bubbly liquids using speed of sound augmented Coriolis technology". In: *Flow Measurement and Instrumentation* (2023). DOI: 10.1016/j.flowmeasinst.2023.102358.

[29] Jaroslav Ivantysyn and Monika Ivantysynova. *Hydrostatic Pumps and Motors: Principles, Design, Performance, Modelling, Analysis, Control and Testing*. Tech Books International, 2003. ISBN: 81-88305-08-1.

[30] Dinghao Pan and Andrea Vacca. "Total Efficiency Prediction of Crescent-Type Internal Gear Pump Considering Floating Balancing Components". In: *ASME/BATH 2023 Symposium on Fluid Power and Motion Control*. Oct. 2023. DOI: 10.1115/FPMC2023-111553.

[31] Fred W. Ocvirk. *Short-bearing approximation for full journal bearings*. Tech. rep. NASA Technical Reports NACA-TN-2808, 1952.

[32] Dinghao Pan and Andrea Vacca. "Modeling of crescent-type internal gear pumps considering gear radial micromotion". In: *Chemical Engineering & Technology, special Issue: Digital, Reliable, Sustainable - Recent Innovations in Fluid Power* (). DOI: 10.1002/ceat.202200419.